European Journal of Pharmaceutics and Biopharmaceutics 107 (2016) 97–109

Contents lists available at ScienceDirect

European Journal of Pharmaceutics and Biopharmaceutics

journal homepage: www.elsevier.com/locate/ejpb

Research paper

Acitretin and aloe-emodin loaded chitin nanogel for the treatment of psoriasis

G. Divya [a], Rajitha Panonnummal [a], Swati Gupta [a], R. Jayakumar [b], M. Sabitha [a,*]

[a] Amrita School of Pharmacy, Amrita Institute of Medical Sciences and Research Centre, Amrita Vishwa Vidyapeetham, Amrita University, Kochi 682041, India
[b] Amrita Centre for Nanosciences and Molecular Medicine, Amrita Institute of Medical Sciences and Research Centre, Amrita Vishwa Vidyapeetham, Amrita University, Kochi 682041, India

ARTICLE INFO

Article history:
Received 23 February 2016
Revised 14 June 2016
Accepted in revised form 24 June 2016
Available online 28 June 2016

Keywords:
Acitretin
Aloe-emodin
Chitin nanogel
Toxicity
Psoriasis

ABSTRACT

The present study focuses on the development of an effective topical nanogel formulation of two anti-psoriatic drugs; Acitretin (Act) and Aloe-emodin (AE) using natural polymer chitin. Simple regeneration chemistry was used to prepare Chitin Nanogel Systems (CNGs). The developed control chitin (CNGs) nanogels, acitretin loaded chitin nanogels (ActCNGs) and aloe-emodin loaded chitin nanogels (AECNGs) were characterized by DLS, SEM, FTIR, XRD and TG-DTA. The systems were found to be spherical in shape with a size range of 98 ± 10, 138 ± 8 and 238 ± 6 nm having zeta potential values of +28 ± 3, +27 ± 3 and +25 ± 6 mV for CNGs, ActCNGs and AECNGs respectively. The *in vitro* haemolysis assay revealed that all the nanogel systems are blood compatible. The systems exhibited higher swelling and release at acidic pH. The *ex vivo* skin permeation studies using porcine skin confirmed the higher deposition of the systems at epidermal and dermal layers, which was confirmed further by fluorescent imaging. The *in vivo* anti-psoriatic activity study using Perry's mouse tail model and skin safety studies confirmed the potential benefit of the system for topical delivery of acitretin and aloe-emodin in psoriasis.

1. Introduction

Psoriasis is a chronic T-cell mediated autoimmune inflammatory skin disease with relapsing episodes of inflammation and hyperkeratosis on the skin. It affects millions of population worldwide, with an equal sex distribution [1]. The general characteristics of psoriasis are sharply demarcated erythematous (red) papules and plaques with adherent silvery scales which affect the skin and also other parts of the body such as joints, nails, scalp and tendons [2]. Even though it is non-contagious, impacts of psoriasis are analogous to those of cancer, heart disease, diabetes, or depression both physically as well as psychologically [3]. Review of literature revealed a prevalence rate of 0.1–8% throughout the world for psoriasis [4]. Although the genetic basis of psoriasis and crucial malfunctions of the innate and adaptive immunity have been emerging as causal factors, therapy is still exclusively symptomatic and a true cure is still elusive [5]. Currently, psoriasis is managed and grounded on the information of its symptoms and affecting factors. Time of incidence, trigger factors, behaviour of disease in different individuals, infuriating factors, and effectiveness of the existing drug as well as availability and cost of therapy will have role in its management [6]. Among the different types of psoriasis, pustular psoriasis is highly inflammatory and recalcitrant type [7–9].

Acitretin (13-*cis*-*trans* retinoic acid), the FDA approved systemic retinoid, has been used from the past decades and is found to be very effective for severe psoriasis, especially for the pustular type [10]. But the use is limited due to its severe systemic toxicity such as teratogenecity. So, it is highly essential to develop a topical formulation of acitretin, which would lower the systemic toxicities associated with the drug by increasing its local availability in the skin. But for formulation scientists, it is a great challenge to

Abbreviations: Act, acitretin; AE, aloe-emodin; CNG, chitin nanogel; ActCNGs, acitretin loaded chitin nanogels; AECNGs, aloe-emodin loaded chitin nanogels; kDa, kilo Dalton; FT-IR, Fourier transforms Infrared spectroscopy; XRD, X-ray diffraction; DMSO, dimethyl sulphoxide; DLS, dynamic light scattering; PBS, phosphate buffered saline; SEM, scanning electron microscope; pH, potenz hydrogen; EE, entrapment efficiency; TG-DTA, Thermo Gravimetric-Differential Thermal Analysis; MTT, [3-(4,5-dimethylthiazol-2-yl)-2,5-diphenyltetrazolium bromide]; ACD, Acid Citrate Dextrose; rpm, revolution per minute; OD, optical density; L929, Mouse dermal fibroblast; HaCaT, human epidermal keratinocytes; DMEM, Dulbecco's modified Eagles Medium; FBS, foetal bovine serum.

* Corresponding author.
E-mail addresses: sabitham@aims.amrita.edu, sabitha.mangalath@gmail.com (M. Sabitha).

http://dx.doi.org/10.1016/j.ejpb.2016.06.019
0939-6411/

develop such a formulation due to the unique problems of the drug such as skin irritation, extremely low solubility and instability in the presence of air, light and heat [11–13].

Aloe-emodin (1, 8-Dihydroxy-3-(hydroxymethyl)-9, 10-anthraquinone) is a natural anthraquinone derivative obtained from the latex of aloe vera plant [14]. It is a non-carcinogenic drug with many medicinal benefits. The anti-inflammatory, anti-viral, anti-proliferative, analgesic and wound healing effects of aloe-emodin are highly beneficial for treating psoriasis [15,16]. Aloe-emodin is one of the active constituents in the marketed liquid formula ProZ92, which is a natural remedy for psoriasis [17]. Hence the chitin nanogel system of aloe-emodin in combination with that of acitretin is expected to produce an additive effect with reduced toxicity of acitretin at lesser dose of both the drugs.

In order to overcome the limitations of acitretin as a topical formulation, numerous efforts have been made and are still under exploration to develop a novel topical vesicular system [18]. Nanogels are favourable and advanced drug delivery systems that can play a vibrant role by addressing these problems associated with the selected drugs [19]. The cationically charged, biodegradable and biocompatible chitin based nanogel system is a good candidate in these aspects, due to its improved skin penetration, enhanced stability and prolonged therapeutic activity [20–22]. Based on these aspects, we developed chitin nanogel system of drugs acitretin and aloe-emodin for the topical delivery in psoriasis.

2. Materials and methods

2.1. Materials

Acitretin was generously gifted by Ranbaxy Pvt Ltd. Aloe-emodin was purchased from Yucca Enterprises, Mumbai and chitin (degree of acetylation-72.4%, molecular weight 150 kDa) from Koyo chemical Co., Ltd, Japan. Calcium chloride dehydrates and dimethyl sulphoxide was purchased from Nice Chemical Pvt. Ltd. India, and Methanol from Spectrum reagents and chemicals Pvt. Ltd., Kochi, India. Iso-propyl Myristate extra pure was purchased from Loba Chemie Pvt. Ltd., Mumbai. Tacroz Forte (Marketed formulation; Tracrolimus ointment 0.1% w/w, Glenmark Pharmaceuticals Ltd, India) was procured from local chemist store. All other ingredients used in the studies were of analytical grade. Millipore water was used throughout the study.

2.2. Experimental

2.2.1. Preparation of control chitin nanogels (CNGs)

Chitin solution (0.5%) was prepared as reported [23,25]. The CNGs were prepared by regeneration chemistry [23]. The optimization of nanogel was done based on amplitude, time of probing, particle size and percentage of drug release [24].

2.2.2. Preparation of Act loaded chitin nanogels (ActCNGs)

This was done by dissolving Act in dimethyl sulphoxide (DMSO) and added to 5 mL methanol to obtain a concentration of 1 mg/5 mL. The resultant solution was added drop by drop to 0.5% chitin solution under constant stirring on a magnetic stirrer. Stirring was continued for 6 h to ensure appropriate loading of the drug. During addition the solution turned turbid yellow. The unentrapped drug was removed by centrifugation and yellow pellet obtained was resuspended in water. Probe sonication was done at 45% amplitude to reduce the particle size and repeated the washing and centrifugation.

2.2.3. Preparation of AE loaded chitin nanogels (AECNGs)

AECNGs were prepared by dissolving AE directly in 5 mL of methanol to obtain a concentration of 2.5 mg/5 mL, which was added to chitin solution for regeneration of AE loaded CNGs. Remaining steps of centrifugation and sonication were followed same as mentioned above.

2.2.4. Preparation of combination nanogels

For preparing combination of ActCNGs and AECNGs half quantity of the final pellets obtained from individually prepared nanogels was mixed together.

2.2.5. Preparation of Rhodamine-B conjugated drug loaded CNGs

Tagging of fluorescent rhodamine-B with the prepared systems was done by adding 40 μL of dye solution (1 mg/mL) to 5 mL of the nanogel system under constant magnetic stirring. The resulting mixture was then probe sonicated and kept for overnight stirring in dark room. The unbound rhodamine was removed by centrifugation at 20,000 rpm for 30 min [25,26].

2.3. Entrapment efficiency (EE)

The supernatant collected after each centrifugation step during the preparation was combined to estimate the EE. Amount of unentrapped drug was quantified by UV spectrophotometry using methanol as blank. The amount of drug in the nanogel systems was calculated using the formula given below (values were triplicated, n = 3) [27].

$$\text{EE } (\%) = \frac{\text{Amount of drug in nanogel}}{\text{Amount of drug taken initially}} \times 100$$

2.4. Characterization

The size distribution and surface charge (zeta potential measurements) of the nanogel systems were studied by DLS (DLS-ZP/Particle Sizer Nicomp TM 380 ZLS). Further SEM (JEOLJSM-6490LA) was used to reconfirm the average size and surface morphology of the nanogel systems. Characterization was further done by FTIR, X-ray diffraction (XRD) and TG-DTA (SII TG/DTA 6200 EXSTAR) analysis.

2.5. Swelling studies

The degree of swelling of CNGs, ActCNGs and AECNGs was studied at pH 4, 7 and 9. The samples kept in the corresponding pH solution for sufficient time, and the dry weight (W_O) and wet weight (W_w) of lyophilized nanogel were determined. The ratio of swelling was calculated using the following equation. The study was triplicated in each pH [23,25,28].

$$\text{Swelling ratio} = [Ww - Wo]/Wo$$

2.6. Rheology of nanogel systems

The rheological properties of nanogel systems were analysed using Brookfield Rheocalc V 32 Rheometer (Brookfield, USA) DV-II model with CP40 spindle using cone and plate geometry. Each sample was equilibrated at 28 °C prior to every measurement and data analysis was done with Brookfield Rheocalc 2.010 Application Software. Viscosity *vs* shear rate as well as the viscoelastic modulus and phase angle *vs* frequency for all the systems were investigated. The measurements were triplicated for each system [29].

2.7. In vitro drug release study for drug loaded nanogels

In vitro drug release studies were conducted at pH 5.5 by cellophane membrane barrier method in orbital incubator shaker at 37 °C and 50 rpm. The final nanogel pellets dispersed in 2 mL of pH 5.5 buffer, which formed the donor fluid. The receptor fluid was a mixture of pH 5.5 buffer and methanol in the ratio 7:3 for ActCNGs and pH 5.5 buffers alone for AECNGs. With the intention to study the effect of one drug on the release pattern of other, the same method was followed for combination of nanogel systems also. This was done by dispersing equal quantity of the pellets of ActCNGs and AECNGs in the same buffer solution. Sink condition was maintained in all the experiments. Samples were withdrawn at predetermined interval from receptor fluid and replaced with fresh buffer. These samples were analysed spectrophotometrically. The quantity of the drug present was calculated and percentage drug release was plotted against time [30,31].

The kinetic modelling was done using the data obtained from release studies. Model fitting into Higuchi and Korsmeyer Peppas was done to study the mechanism behind the release pattern.

2.8. Ex vivo skin permeation studies

Skin permeation study was conducted using porcine ear skin. In vertical Franz diffusion (FD) cell, skin was mounted in the donor compartment and the temperature was maintained at 32 ± 1 °C for a period of 24 h [23,25]. The cumulative amount of drug permeated as well as the permeation flux was determined for control solution of drugs, drug loaded systems and for combination system of drugs. The receptor fluid used for control solution (Act in isopropyl Myristate) and nanogel system of Act was a mixture of pH 5.5 buffer and methanol (7:3). In case of AE it was pH 5.5 buffer alone. The amount of drug permeated was quantified from the collected aliquots at predetermined intervals using UV spectroscopy. All the values were triplicated.

2.9. Drug retention studies

The skin samples (1 cm^2 area) of permeation study were collected in triplicate. These samples were fixed on cork disc using tissue freezing medium, sectioned using cryotome (LEICA CM 1510S) into different layers as stratum corneum, epidermis and dermis. These sections were incubated in 100 μL of methanol overnight. The supernatant was collected after centrifugation and drug present was determined spectrophotometrically. Amount of drug present in μg/cm^2 of skin *vs* different skin layers was plotted [23,25,32].

2.10. Fluorescent imaging of Rhodamine-B tagged systems

Ex vivo skin permeation experiments for Rhodamine-B tagged nanogel systems were conducted to confirm the drug localization at different depths of skin layers. After proper washing, the skin samples were cryo-sectioned. The selected sections were treated with xylene for water removal. Then it was mounted on to the glass slide using DPX for fluorescent imaging and viewed under the fluorescent microscope (Olympus-BX-51) [23,25].

2.11. In vitro haemolysis assay

Fresh human blood was used to evaluate the blood compatibility of formulations by *in vitro* haemolysis. Blood samples were collected in tubes containing Acid Citrate Dextrose (ACD) as anticoagulant. To 1 mL of this blood sample, 100 μL of nanogel system at different concentrations (0.1–1 mg/mL) was added and incubated in an orbital shaking incubator kept at 37 °C with 50 rpm for 2 h. Plasma was separated by centrifugation for 10 min at 4500 rpm. 100 μL of this was mixed with 1 μL of 0.01% Na_2CO_3. The optical density (OD) values were read using microplate reader at 450, 380 and 415 nm. The plasma haemoglobin was calculated using the equation given below [32].

$$\text{Plasma Hb} = \{(2A_{415}) - [A_{380} + A_{450}] - 76.25\}$$

The obtained values of samples compared with that of positive control (Triton X) and negative control (normal saline). The values were triplicated.

2.12. Cytotoxicity studies

Mouse dermal fibroblast (L929, NCCS Pune) cells and Human epidermal keratinocytic (HaCaT) cells were used to evaluate the cell toxicity of the formulated systems [33]. The cells maintained in Dulbecco's modified Eagles Medium (DMEM) supplemented with 10% foetal bovine serum (FBS) was cultured in culture flask and kept in CO_2 incubator maintained at 5% CO_2 till reaching confluency. Then the cells were detached from the flask with Trypsin-EDTA and centrifuged at 1200 rpm for 5 min. This was re-suspended in the growth medium for further study. Cytotoxicity experiments were carried out on these cell lines by MTT [3-(4, 5-dimethyl-thiazole-2-yl)-2, 5-diphenyl tetrazolium] assay. This colorimetric assay is based on the conversion of MTT to formazan crystals (purple colour) by the mitochondrial reductase enzyme present in viable cells. The 96 well plates were seeded with a density of 10,000 cells/cm^2. Concentration ranging from 0.1 to 0.25 mg/mL of CNGs, ActCNGs, AECNGs and control drug solutions were prepared by diluting with the medium. After reaching 90% confluency, the cells were washed with PBS buffer and various concentrations of the prepared CNGs suspension (100 μL) were added into it and incubated for 24 h. The cells in medium served as the negative control and Triton X-100 treated cells as the positive. Then these cells were treated with MTT for 4 h to form formazan crystals. The formazan crystals were then dissolved by adding100 μL of solubilization buffer and the optical density was measured using a Beckmann Coulter Elisa plate reader (BioTek Power Wave XS) at a wavelength of 570 nm. The samples were triplicated.

2.13. Stability studies

The nanogels systems were filled in glass wares and incubated at 2–8 °C (refrigeration condition), room temperature (30 ± 2 °C) and at 40 °C/65% RH (accelerated condition) for 90 days [34]. The physical stability of the formulation was examined visually for appearance, colour and odour in every 30 days. The change in particle size and the drug content of the system was also estimated using DLS (Nicomp 380 ZLS) and UV spectrophotometer respectively.

2.14. In vivo studies

Adult Swiss albino mice (weight: 30–35 g) were procured from Central lab animal facility, AIMS, Kochi, under IAEC approval with reference no: IAEC/2014/2/2. They were grouped and housed (n = 6/cage) in wire mesh cage one week prior to the study in order to acclimatize them with the laboratory conditions (temperature at 22 ± 2 °C and RH at 50 ± 15%). Animals were pellet fed and water supplied *ad libitum*. They were taken care as per the guidelines of CPCSEA.

2.14.1. Evaluation of anti-psoriatic activity using mouse tail model

Perry scientific mouse tail model is considered as one of the accepted psoriasis model [35–40]. Investigation on this model is

based on the fact that the adult mouse tail normally has parakeratotic differentiation, which is the hallmark of psoriasis. So, the hypothesis that, when the mouse tail is treated topically with the nanogel systems of anti-psoriatic drugs the parakeratotic differentiation changes to orthokeratosis (OK). The induction of orthokeratosis was examined microscopically. Measurement of the epidermal thickness was also taken using Image J software to determine efficacy of the systems.

The animals were grouped into six as shown below. From group 2 to 6, the formulations were applied on the proximal half of the tail (2 cm long) once daily for a period of 30 days. After two hours of last treatment, animals were sacrificed and the entire dosing area was stripped off from the underlying cartilage. The processed skin was kept in formalin solution for a period of three days to ensure fixing. Longitudinal sections of about 5 μm thicknesses were cut, stained using haematoxylin and eosin for histological evaluation.

- Group 1: Control
- Group 2: CNGs
- Group 3: ActCNGs
- Group 4: AECNGs
- Group 5: Combination (ActCNGs + AECNGs)
- Group 6: Standard (Tacrolimus 0.1% cream)

2.14.2. Skin irritation study

Adult Swiss albino mice were used to test the irritation potential of the nanogel systems [39]. The hair on the dorsal side was removed using animal clipper (0.1 mm). This area was wiped with wet cotton swab and the nanogel system of CNGs, ActCNGs, AECNGs were applied topically on the prepared area. One group was left as control. After 24 h exposure, the dosing area was cleaned and examined for visual changes. Then they were sacrificed, the skin samples were collected and stored in formalin for three days for fixation. The samples were stained for histological examination to compare the changes with that of the normal control skin.

2.15. Statistics

All data are expressed in mean ± standard deviation after triplicate sample analysis. Statistical significance was assessed by Paired Student's two-tailed *t* test, wherever necessary and applicable. A value of $p < 0.05$ is considered to be statistically significant.

3. Results and discussion

3.1. Preparation of drug loaded nanogels

CNGs were obtained by the regeneration of chitin on addition of excess methanol. The mechanism behind the formation of drug loaded nanogel systems could be the interplay between the chitin functionalities (—OH and —$NHCOCH_3$) to that of the drug [40]. In ActCNGs, the active groups of the highly lipophilic drug Act (—OH, —C═O and —$COCH_3$) bind through strong hydrogen bonds *via* end to end interaction [41]. In AECNGs, the possible interaction of hydrophobic drug AE with polymer chitin can be due to strong hydrogen bonding between 3 hydroxyl groups of drug with the terminal functionalities of chitin [42]. The stability of nanogel is contributed by the hydrophobic interaction of chitin functionalities. Since both the drugs are hydrophobic in nature and encapsulated during the process of regeneration, the stability is expected to be higher [43]. The formulations of ActCNGs and AECNGs are shown in Fig. 1A and B.

3.2. Entrapment efficiency (EE)

The EE of ActCNGs was found to be ~94% and that of AECNGs was ~89%. In previously reported system of Act loaded Nanostructure Lipid Carriers (ActNLCs) the EE showed was only 63% [18]. In

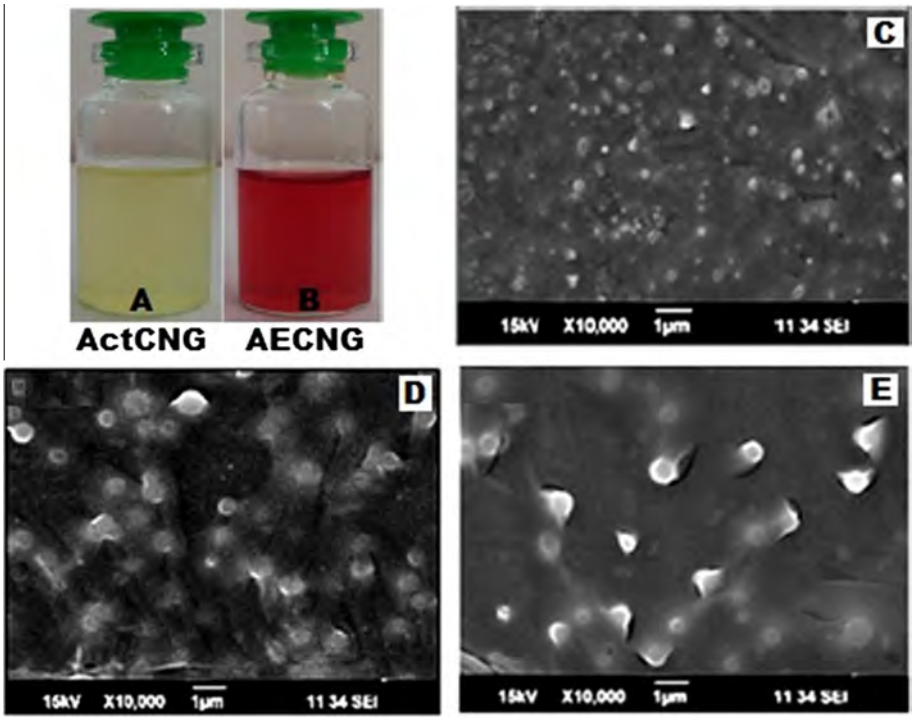

Fig. 1. Formulation of ActCNGs (A), AECNGs (B) and SEM images of CNGs (C), ActCNGs (D) and AECNGs (E).

the present study, the better EE of Act in CNGs can be due to the entrapment of drug during the regeneration of CNGs. EE was directly proportional to the amount of drug added and incubation time, which indicates the critical effect of drug concentration and time of incubation on it.

3.3. Characterization

3.3.1. Size and surface morphology

The size and surface morphology of CNGs, ActCNGs and AECNGs was studied by DLS and SEM. The systems showed a size range of 98 ± 10, 138 ± 8 and 238 ± 6 nm respectively with spherical morphology (Fig. 1C–E). The size of the drug loaded systems was found to be larger than CNGs. This can be due to the encapsulation of drug within the carrier system. The SEM images revealed almost spherical particles uniformly distributed without any aggregation. The stability of the prepared nanogel systems was analysed by zeta potential measurements and the values were found to be +28 ± 3, +27 ± 3 and +25 ± 6 mV for CNGs, ActCNGs and AECNGs respectively. Zeta potential value closer to +30 mV (limit of stable preparation) suggesting the stability of the systems and the positive charge was attributed by cationic chitin. From the above studies all systems were found to be of nanosize, spherical shape (Fig. 1) and with positive charge which could be highly favourable for efficient transdermal penetration through the complex skin barrier [44] (see Table 1).

Table 1
Formulation parameters.

Samples	Drug used (mg)	Probing time (min)	Probing amplitude (%)	Particle size (nm)	Entrapment efficiency (%)
CNGs	–	5	75	98 ± 10	–
ActCNGs	1	5	75	138 ± 8	94 ± 3
AECNGs	1.25	5	75	238 ± 6	89 ± 2

3.3.2. FTIR analysis

The FTIR analysis was done to study the potential chemical interaction between the drug and the CNGs, which is showed in Fig. 2A. FTIR spectra of chitin and CNGs have characteristic peaks at 3500–3400, 1640 (amide I region) and 1070 cm^{-1} (—C—O— stretching), which was already reported by our group in many past studies [23,25]. Act was characterized by peaks around 1700–1500 and 1300–1000 cm^{-1} [45]. Peaks at 1676 and 1624 cm^{-1} contributed by amide I region and —C=C— stretching respectively. The bands appeared at 1300–1000 cm^{-1}assigned to the stretching vibrations of —C—O groups. The spectra of ActCNGs showed retention of the characteristic peaks of Act and showed shifts corresponding to —OH stretching from 2976 of Act to 3490 cm^{-1} (characteristic peak of CNGs). An additional peak at 3248 cm^{-1} with broadening may be due to the intermolecular hydrogen bonding between Act and CNGs. AE was characterized by peaks at 1676 and 1631 cm^{-1} assigned to free —C=O group and conjugated —C=O group, respectively. Peaks at 1476 and 1288 cm^{-1} are assigned to the skeletal ring stretching vibration frequencies [46]. However, spectra of AE loaded nanogel showed broadened band at 3488 cm^{-1} assigned to —OH stretching (characteristic peak of CNG) and an additional peak formed at 3250 cm^{-1} confirmed the conjugation of drug with nanogel by intermolecular hydrogen bonding.

3.3.3. XRD analysis

The XRD pattern of chitin revealed the amorphous nature which improved after conversion into CNGs. This improvement attributes to the presence of residual calcium ions present in CNGs. Acts showed its characteristic peaks between 9.39 and 12.44° [47], but ActCNGs did not show any protruding crystalline peaks as in drug. The reason could be the intermolecular interaction between drug and amorphous chitin within the CNG matrix. This reveals the complete entrapment of Act inside the CNGs. In the diffractogram of AECNG some of the peaks of AE were absent, which indicates the decrease in crystalline nature of AE in AECNGs [48]. This further

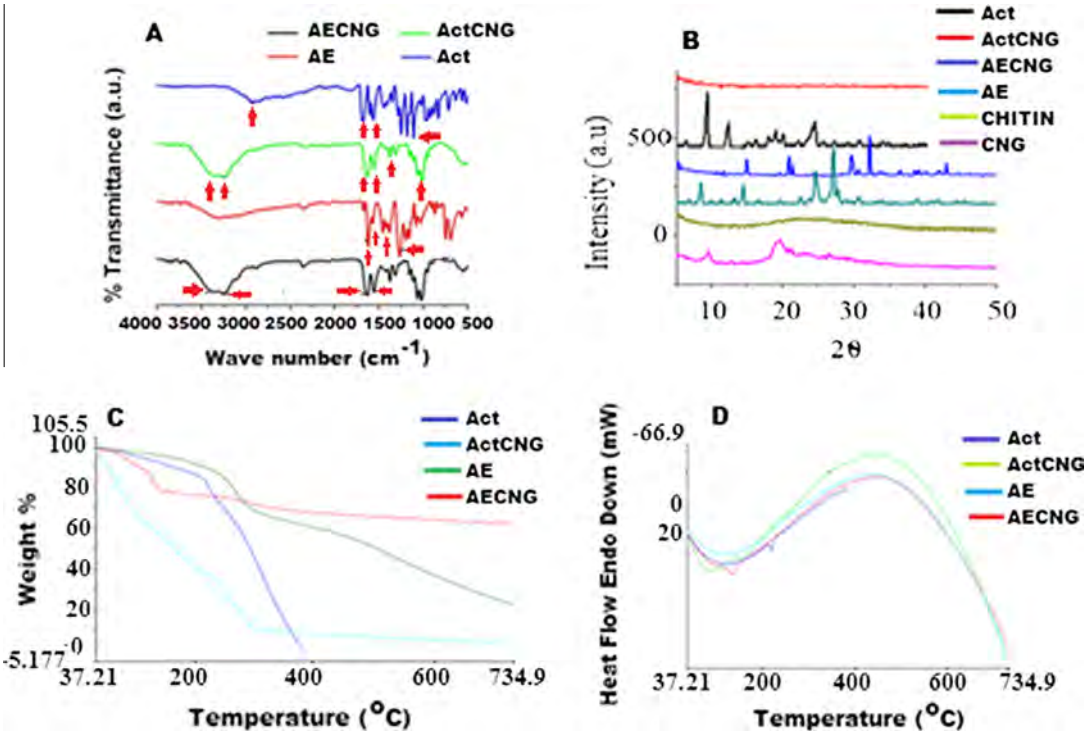

Fig. 2. FTIR spectra (A) XRD analysis (B) TG (C) and (D) DTA of the systems.

confirms the improved stability of drug inside CNGs. The diffractogram is shown in Fig. 2B.

3.3.4. Thermo Gravimetric and Differential Thermo Gravimetric Analysis

The TG-DTA of chitin and CNGs has already been reported by our group [23,25]. The TG of Act and AE (Fig. 2C) revealed the stability of the drugs up to their melting point at 229 and 223 °C respectively, after which the degradation started. In case of ActCNGs and AECNGs, the degradation was much faster compared to the control drugs. In ActCNGs almost 75% of the degradation happened before its melting point. In AECNGs, the degradation occurs in two stages, almost 50% happened before 150 °C and 75% before 300 °C. This could be attributed to the faster degradation property of CNGs as reported [24].

The DTA of Act shows an endothermic peak at 229 °C, which corresponds to its melting point. The DTA of ActCNGs shows several endothermic peaks between 77 and 280 °C. This is due to the complex degradation of drug loaded nanogel. The DTA of AE (Fig. 2D) shows an endothermic peak at 223 °C, which corresponds to the melting point of the drug. But the endothermic peak of AECNGs in DTA thermogram showed a shift from 223 to 89 °C. This shift shows the faster degradation of chitin nanogel which could be due to the water evaporation.

3.4. Swelling studies

The swelling ratio of bare and the drug loaded systems were found to be greater at acidic pH than neutral and alkaline pH as shown in Fig. 3A. Usually polyelectrolyte gels swell at pH below its pK_a, which of chitin is 6.1 [49,50]. The swelling of drug loaded nanogels was found to be lesser than bare nanogels, which could be due to the less number of free reactive functionalities in these since they are conjugated with drug.

3.5. Rheology

Rheological studies (Fig. 3B and C) showed a decrease in viscosity with increase in shear rate at 25 °C, indicate the shear thinning and thixotropic behaviour of pseudo plastic (non-Newtonian) system. An elastic modulus value greater than the viscous modulus suggests the elastic gel like behaviour of the systems. The phase angle value less than 40° (range is 0–40° for gels) confirms the gel like behaviour of the developed system for topical application [29].

3.6. In vitro release study of drug loaded nanogels

The *in vitro* release of Act and AE from the systems alone as well as from the combination systems were studied (Fig. 3D and E).

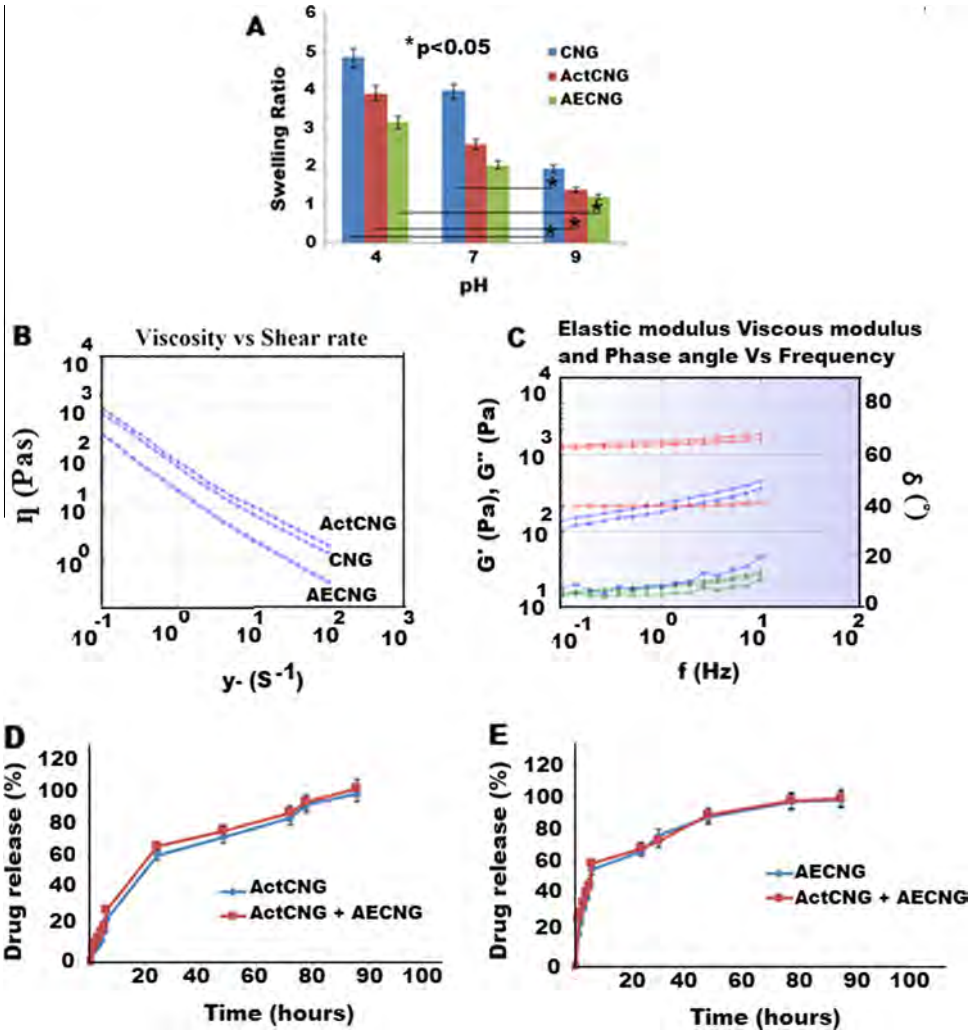

Fig. 3. Swelling index at different pH (A), Rheological study for Viscosity *vs* shear rate (B) and Elastic-Viscous modulus *vs* frequency (C), Percentage release of Act from ActCNGs and Combination (D) and AE from AECNGs and Combination (E).

About 60% of Act released at 24th h from ActCNGs and was found to increase up to 96% at 96th h. The same release pattern was followed by Act from the combination system also. The release of AE from AECNGs and from combination was found to be 68% and 98% at 24th h and 96th h respectively. The higher release at pH 5.5 is attributed to increased swelling of the system at this pH possibly due to the protonation of free amine groups [23,25].

3.6.1. Kinetic analysis

Kinetic study revealed that both Act and AE loaded CNGs follow a first order release pattern. From model fitting to Higuchi and Korsmeyer-Peppas, release mechanism was found to be a combination of simple diffusion, nanogel degradation and the displacement by counter ions present in the environment. This can be due to the ionization of the pendant groups in the nanogel network. This causes electrostatic repulsion between the like charges leading to the expansion of pores, permitting excess solvent influx and ends up with the release of encapsulated payload [51]. The n values from Korsmeyer-Peppas model shows that the drug release pattern follows anomalous transport (non-Fickian) mechanism. Data is showed in Table 2.

3.7. Ex vivo skin permeation studies

The cumulative amount of drug permeated per cm^2 of skin was determined (Fig. 4A and B). From the permeation study of Act, ActCNGs (268.34 ± 5.56 μg/cm^2) showed two fold increased permeation than that of control Act solution and the same was observed in case of combination too with $p < 0.05$. In case of AE, cumulative amount was more for AECNGs (350 μg/cm^2) and combination ($p < 0.05$) compared to that of control AE in methanol. The major parameter influencing the penetration is the nanosize of the system, cationic charge as well as the hydrophobicity of the polymer. Greater will be the interaction of positively charged chitin with negatively charged skin lipids, if the polymer is more cationic [25]. The hydrophobic nature of drug moieties further increased the hydrophobicity of chitin carrier. So the interaction will be enhanced with the hydrophobic areas of keratin in the corneocytes through van der Waals force, which results in disruption of keratin within the corneocytes and causes increase in diffusion coefficient [52]. Loosening of organized epidermal layers with fragmentation of stratum corneum in pig ear skin treated with chitin nanogel is previously reported by our group [23]. This is another factor facilitating the improved permeation via transdermal penetration.

Table 2
Kinetic modelling data.

Formulations	Zero order R^2	First order R^2	Higuchi R^2	K-Peppas	
				R^2	n
ActCNGs	0.866	0.988	0.939	0.905	0.609
AECNGs	0.798	0.819	0.933	0.920	0.841

3.8. Drug concentration-depth profile

The quantity of drug retained in different layers of the skin (stratum corneum, epidermis and dermis) was studied for control solution and drug loaded systems. From the graph of concentration-depth profile (Fig. 4C and D), it is clear that the drug retention for drug loaded nanogel system is more in the derma-epidermal layers than that of control drug solution. In case of ActCNGs the amount of drug retained in epidermis and dermis was found to be 46.64 and 74.42 μg/cm^2 respectively, which indicates that the retention is more in deeper dermal layer of skin. The amount of AE retained in these layers is 92.73 and 126.06 μg/cm^2 respectively, which is much greater when compared with control AE solution.

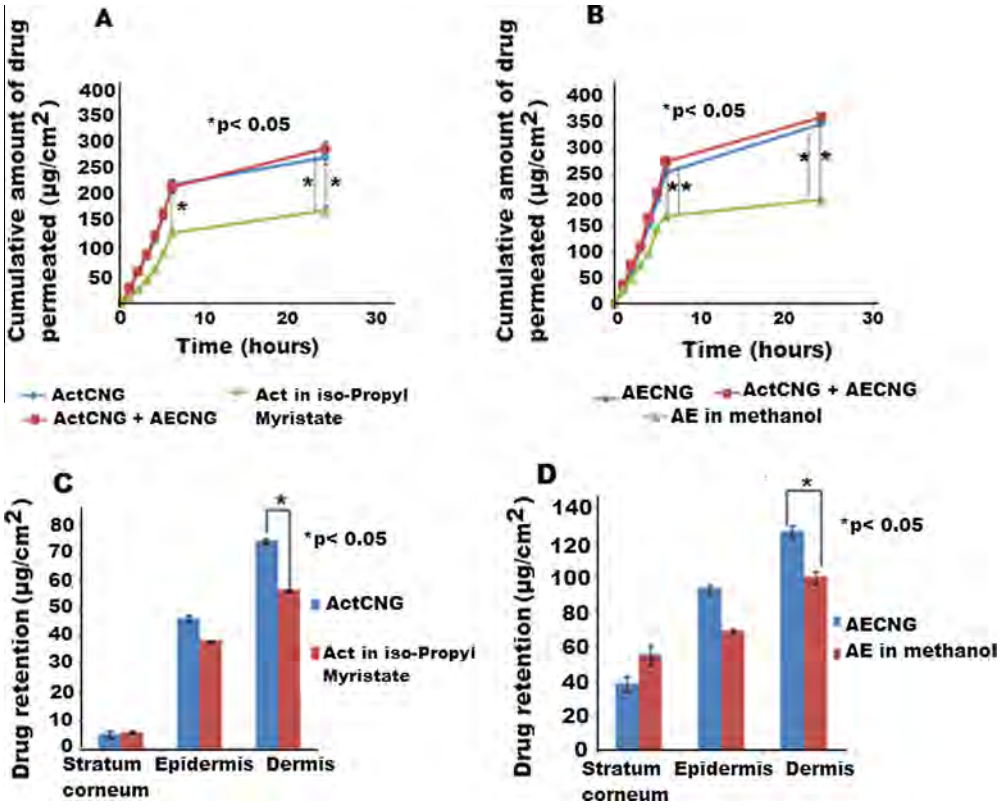

Fig. 4. *Ex vivo* permeation studies of Act (A) and AE (B), drug retention profile of nanogel systems in different layers of the skin (C and D).

3.9. Fluorescent imaging of Rhodamine-B tagged systems

From the fluorescent images of Rhodamine-B conjugated nanogel systems shown in Fig. 5, the high retention of drug at dermal and epidermal layers of skin was reconfirmed. This can be due to the interaction of positively charged chitin with negatively charged skin lipids at these deeper layers [23], which facilitates skin penetration and is highly beneficial for psoriatic skin treatment. Greater accumulation of loaded moieties in deeper layers of the skin indicates that the system can be used for psoriasis therapy, since the major pathological changes in psoriasis happen in these layers.

3.10. Blood compatibility studies

Ex vivo skin retention study revealed the greater retention of drug loaded nanogels in vascularised layer of epidermis suggesting the possibility of drugs to reach into the systemic circulation. So we conducted hemocompatibility assay. The results from *in vitro* haemolysis assay (Fig. 6A and B) revealed that there is no risk of

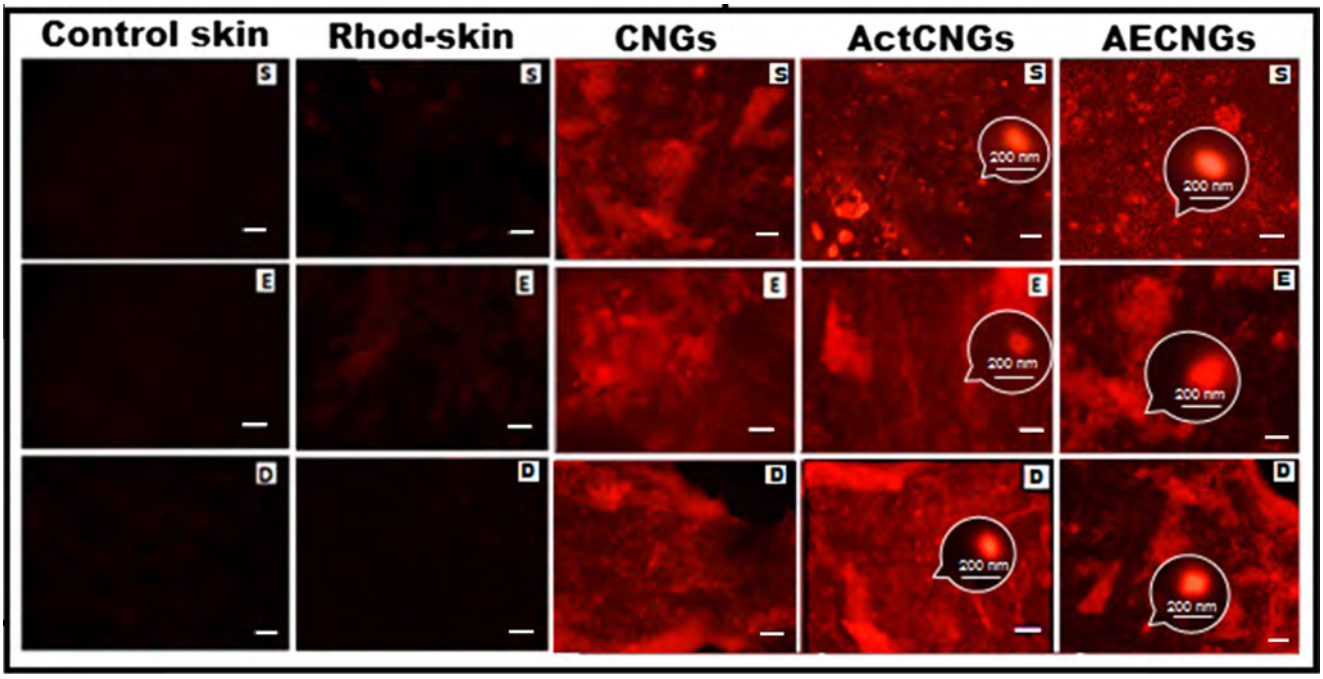

Fig. 5. Fluorescent images of skin treated with CNGs, ActCNGs as well as AECNGs by fluorescent imaging, where 'S' is Stratum corneum, 'E' is Epidermis and 'D' is Dermis. Scale bar indicates 10 μm.

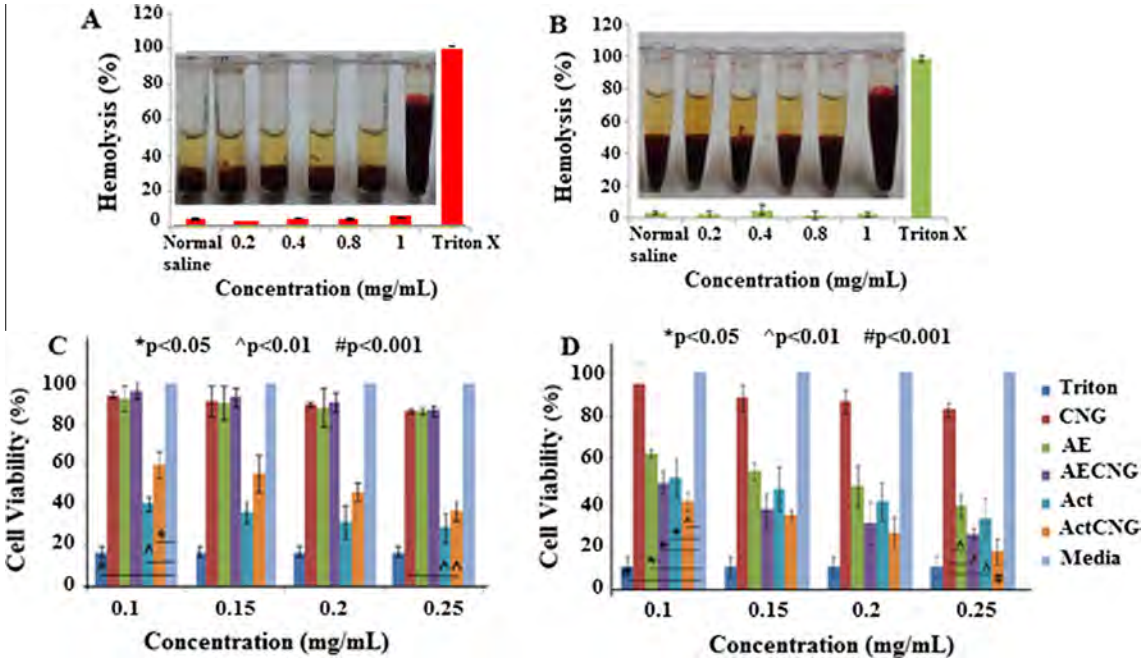

Fig. 6. Percentage Haemolysis of different concentrations of ActCNGs (A) and AECNGs (B) in human blood, Cytotoxicity studies of nanogel systems on L929 (C) and HaCaT (D) cell line by MTT assay.

haemolysis or coagulation even if systemic delivery of ActCNGs or AECNGs at high concentration is achieved through the transdermal route. After the encapsulation of drug in CNGs, the haemolytic percentage was found to be less than 5%, which is the safety margin for biomaterials according to ISO/TR 7406 [23,27].

3.11. Cytotoxicity studies

Cytocompatibility of all prepared nanogel formulations were evaluated using MTT assay on L929 (Mouse dermal fibroblast) cells and HaCaT (Human epidermal keratinocytic) cell lines. Fig. 6C and D shows the graph of the percentage cell viability on L929 cells against different concentration (0.1–0.25 mg/mL) of the prepared systems. The non-toxicity of chitin nanogel towards a number of normal cells has already been reported by our group [23–27]. The cytoprotective action of the natural drug AE on L929 cells is reported previously [53,54]. MTT assay on HaCaT cell line revealed the specific toxicity of AE towards keratinocytic cells, which is further increased after encapsulating in the nanogel system. This can be due to the induction of p21 and p53 genes by released AE which causes cell cycle arrest at G1 phase leading to apoptosis [55,56]. Even though some authors have demonstrated the non-cytotoxic effect of Act towards normal cells, our data on L929 cell elucidate the reduced cell viability of the drug. But it was found to be improved after encapsulation of the drug into CNGs. In fact, the drug showed specific toxicity towards the highly proliferative HaCaT cells at the same concentration range, which was further increased after encapsulating in the nanogel systems. The nanogel may be taken up by the cells by an active uptake process and the released Act will act on the retinoid receptors interfering DNA synthesis leading to cell death [57,58]. Thus the MTT results throw light on the fact that AECNGs show specific toxicity towards human keratinocyte cells without affecting the normal cells, whereas Act and ActCNGs showed higher toxicity towards keratinocyte cells as compared to normal cells. The samples were triplicated for each concentration (mean ± SD, n = 3; $p < 0.05$).

3.12. Stability study

The stability study at different conditions is shown in Fig. 7A and B. The change in size was 30 ± 9, 85 ± 12 and 100 ± 15 nm at refrigerated temperature, RT & elevated temperature respectively. There was no significant change in particle size and drug content when the system stored at refrigerated condition for a period of three months. In fact there was significant increase ($p < 0.05$) in particle size at accelerated condition than refrigerated condition in the same period. During storage at elevated temperature, the enhanced viscoelastic property of the nanogel and collision between the particles, facilitated adhesion and in turn aggregation resulted in increased size [59]. The percentage drug content was also significantly decreased in case of AECNGs at elevated temperature conditions. These results suggest that the optimum storage condition for CNGs system is refrigerated condition.

3.13. In vivo anti-psoriatic activity studies

It is reported that psoriasis is characterized by the hyper proliferation and abnormal differentiation of apoptotic cells, keratinocytes [37]. Numerous experimental animal models have been developed for psoriasis. Some of them are flaky skin mouse [60], asebia mouse [61], ultraviolet ray-B induced photo dermatitis model [62], genetically modified models of psoriasiform skin

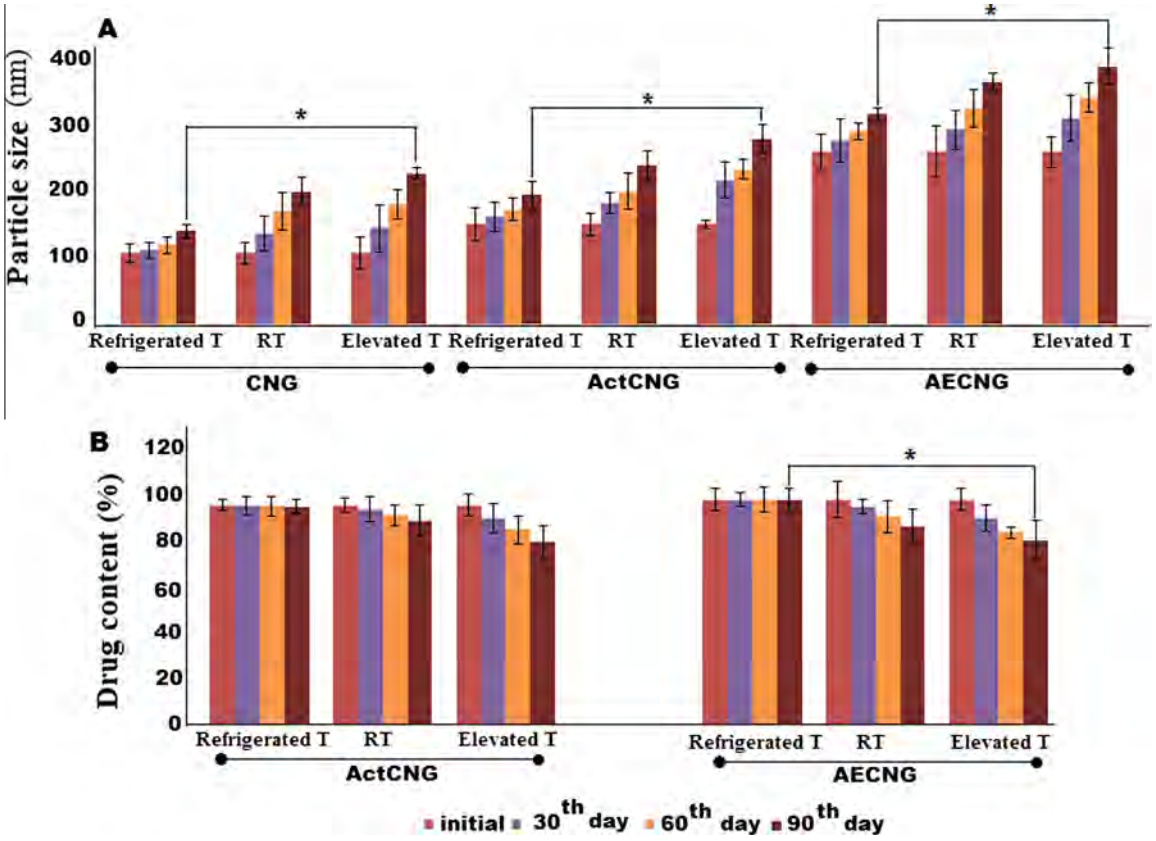

Fig. 7. Stability study for particle size variation (A) drug content changes (B) at 2–8 °C (refrigeration condition), room temperature (30 ± 2 °C) and at 40 °C/65% RH (accelerated condition) for 90 days. Mean ± SD, n = 3; $p < 0.05$.

diseases [63] and mouse tail model [35–38]. Here, the efficacy of the developed systems was studied *in vivo* using mouse tail model. Usually the histopathological changes observed in fully developed lesions of psoriatic skin are prominent parakeratosis, Munro micro abscess, and thickened epidermis, regular elongation of rete ridges along with capillary loop dilatation and absence of granular layer [38]. The features observed in the photomicrographs (Fig. 8) of psoriatic mouse tail skin (control group) are parakeratotic differentiation with thickened epidermis, regular elongation of rete ridges along, capillary loop dilatation and absence of granular layer.

In case of group treated with bare CNGs, the features observed in control skin were retained with slight decrease in epidermal thickness. The reduction in epidermal thickness can be due to the anti-inflammatory action of chitin polymer, as reported earlier.

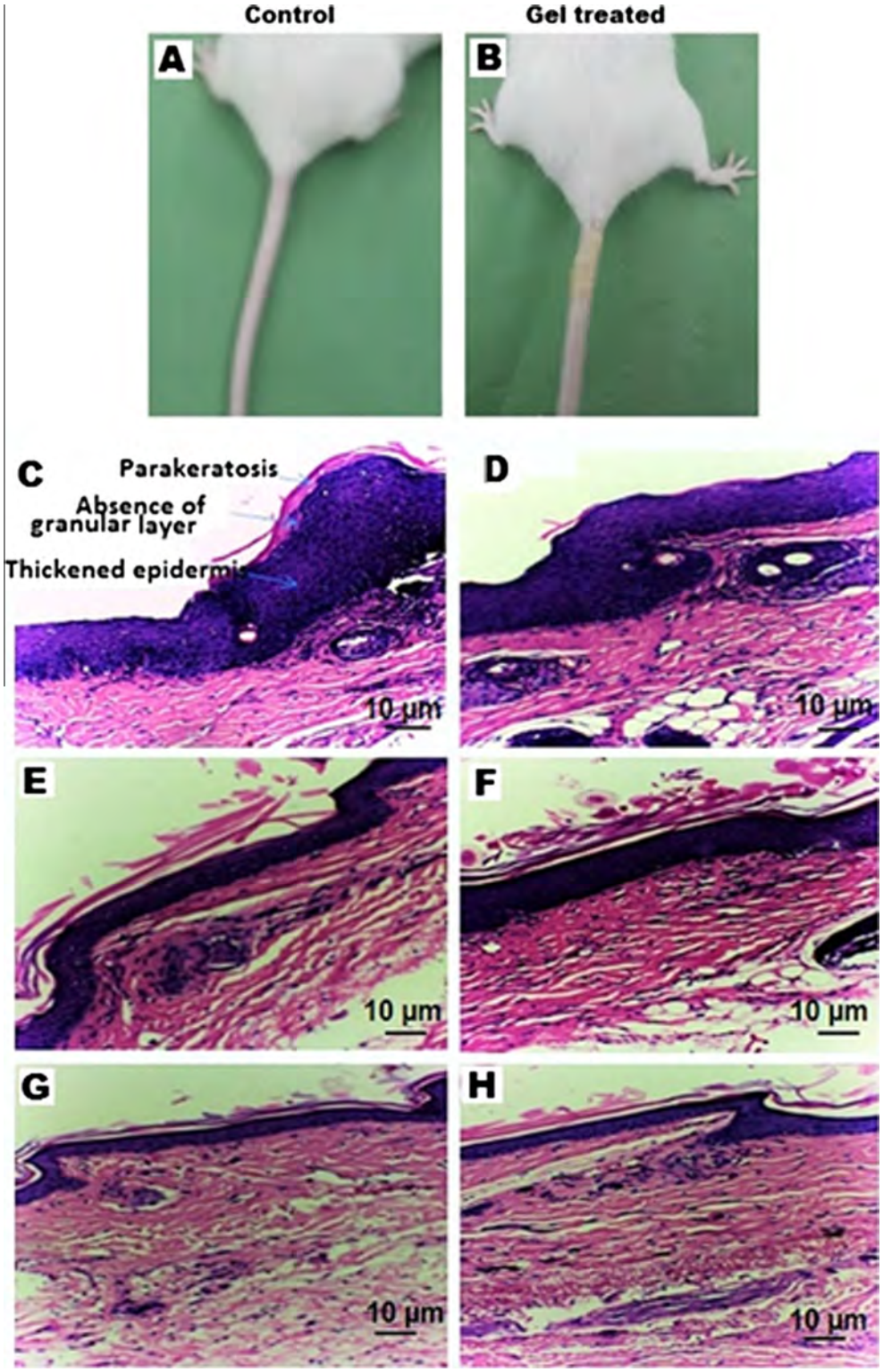

Fig. 8. Photographs of mouse tail Control (A), CNGs (B) and histopathological images of Control tail skin (C), CNGs treated (D), ActCNGs treated (E), AECNGs treated (F), Combination treated (G) and Marketed (Tacrolimus) cream treated (H).

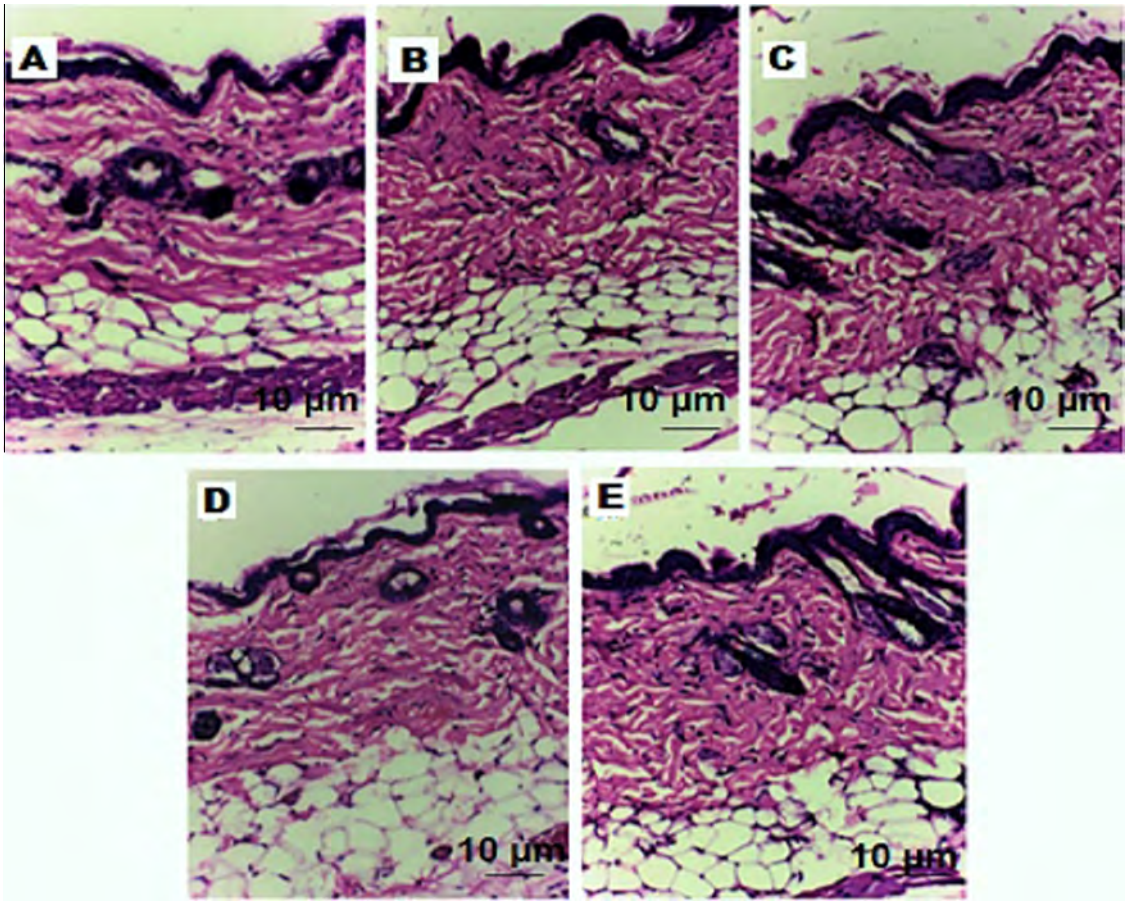

Fig. 9. Photomicrographs of histopathological evaluation of skin irritation studies Control skin (A), CNGs treated skin (B), ActCNGs treated skin (C), AECNGs treated skin (D) and Combination treated skin (E).

Compared to control group, the groups treated with ActCNGs and AECNGs showed induction of orthokeratosis (normal pattern of keratinization) in the region previously observed with parakeratosis (abnormal pattern of keratinization with absence of granular layer). The absence of capillary loop dilatation and regular elongation of rete ridges was remarkable, along with the formation of granular layer. Compared to control group, the epidermal thickness, measured using Image J software shown marked reduction in ActCNGs and AECNGs group, 69% and 56% respectively. Further the group received combination of drug loaded nanogels showing absence of all the characteristic features observed in normal psoriatic rat tail skin sections. In addition, a significantly high reduction in epidermal thickness (86%) showed by this group, which was comparable to that of the group treated with marketed cream, i.e. 87% (tacrolimus cream) These data reveal that ActCNGs has better anti-psoriatic activity than AECNGs, further the system when combined at lesser doses of drugs showed much better effect in this psoriatic model. Hence this study suggests the potential benefits of the drugs in combination for the treatment of psoriasis.

3.14. Skin irritation test

Skin irritation study is a prerequisite for any topical formulation and this is more important in considering the irritability of the drug Act. Even AE is reported to cause mild skin irritation in some patients. Photomicrographs of skin irritation study (Fig. 9) reveal that CNGs, ActCNGs, AECNGs and combination did not produce any histopathological changes on skin like erythema and wrinkles as compared to that of control and commercial formulation. Hence, this study supports the hypothesis that chitin nanogel can be used as a suitable carrier for the drugs like Act and AE for the topical treatment of psoriasis.

4. Conclusion

Drug Act and AE were effectively entrapped in the CNG systems for psoriasis treatment. Particle size was optimized by changing time and amplitude of probing and the optimized systems were selected using particle size and entrapment efficiency. The developed systems of ActCNGs and AECNGs were characterized by SEM, FTIR, XRD and TG-DTA which confirmed the nanosized spherical particles with intermolecular hydrogen bonding. The systems were found to be pH responsive with high swelling at acidic pH and showed thixotropic behaviour of pseudo plastic (non-Newtonian) system. The *in vitro* drug release at pH 5.5 suggested the prolonged release of drug with non-Fickian release pattern. The systems showed greater skin permeation and were hemocompatible. The drug retention was higher at the deeper layers of skin, which is essential to treat disease such as psoriasis. The *in vivo* anti-psoriatic activity study of the nanogels on Perry's mouse tail model confirmed the benefit of the nanogel formulations alone and also the additive effect of nanogel combination system. The histopathological examination after *in vivo* skin irritation study confirmed their biocompatibility. Thus the anti-psoriatic drugs such as Act and AE loaded chitin nanogel systems have proven to be an ideal candidate for transdermal delivery in the dreadful disease psoriasis. The systems were found to be more stable at refrigerated condition as per the stability study.

Acknowledgements

The author Dr. M. Sabitha is thankful for the financial support provided by Department of Science and Technology (DST- FAST TRACK- SB/YS/LS-124/2013), Government of India and Kerala State Council for Science and Technology for their financial support (File No. 104/SPS/2014/CSTE). R. P is thankful towards DST for the financial support through INSPIRE fellowship scheme (IF120499). D. G is grateful to Ranbaxy, India for providing gift sample of Acitretin. The great support from all colleagues at Amrita Center for Nanosciences and Molecular Medicine and Amrita School of Pharmacy is also acknowledged.

References

[1] L. Flatz, C. Conrad, Role of T-cell-mediated inflammation in psoriasis: pathogenesis and targeted therapy, psoriasis, Targets Ther. 3 (2013) 1–10.
[2] M. Pradhan, D. Singh, M.R. Singh, Novel colloidal carriers for psoriasis: current issues, mechanistic insight and novel delivery approaches, J. Control. Release 3 (2013) 380–395.
[3] D.S. Dubois, R. Pouliot, Promising new treatments for psoriasis, Sci. World J. (2013) 980419.
[4] P. Gisondi, G. Malara, M. Ardigo, The psoriatic patient profile for infliximab, Eur. Rev. Med. Pharmacol. Sci. 15 (2011) 1445–1451.
[5] R.K.H. Mak, C. Hundhausen, F.O. Nestle, Progress in understanding the immunopathogenesis of psoriasis, Actas dermo-sifiliograficas 100 (2009) 2–13.
[6] Y. Zheng, D.M. Danilenko, P. Valdez, I. Kasman, J. Eastham-Anderson, J. Wu, W. Ouyang, Interleukin-22, a T(H)17 cytokine, mediates IL-23-induced dermal inflammation and acanthosis, Nature 445 (2007) 648–651.
[7] P.B. Liao, R. Rubinson, R. Howard, G. Sanchez, I.J. Frieden, Annular pustular psoriasis-most common form of pustular psoriasis in children: report of three cases and review of the literature, Pediatr. Dermatol. 19 (2002) 19–25.
[8] E.A. Brezinski, A.W. Armstrong, Strategies to maximize treatment success in moderate to severe psoriasis: establishing treatment goals and tailoring of biologic therapies, Semin. Cutan. Med. Surg. 33 (2014) 91–97.
[9] K.M. Varman, N. Namias, C.I. Schulman, L.R. Pizano, Acute generalized pustular psoriasis, von Zumbusch type, treated in the burn unit. A review of clinical features and new therapeutics, Burns 40 (2014) 35–39.
[10] M. Sevrain, M.A. Richard, T. Barnetche, M. Rouzaud, A.P. Villani, C. Paul, M. Beylot-Barry, D. Jullien, S. Aractingi, Treatment for palmoplantar pustular psoriasis: systematic literature review, evidence-based recommendations and expert opinion, J. Eur. Acad. Dermatol. Venereol. 28 (2014) 13–16.
[11] C. Surber, K.P. Wilhelm, D. Bermann, H.I. Maibach, In vivo skin penetration of acitretin in volunteers using three sampling techniques, Pharm. Res. 10 (1993) 1291–1294.
[12] K. Lauren Dunn, R. Laini Gaar, A. Brad Yentzer, L. Jenna, R.F. Steven, Acitretin in dermatology: a review, J. Drugs Dermatol. 10 (2011) 772–782.
[13] P. Marta, K. Andrzej, Acitretin, a systemic retinoid for the treatment of psoriasis-current state of knowledge, Postep. Dermatol. Alergol. 4 (2011) 285–292.
[14] Hsiu-Mei Chiang, Lin Ya-Tze, H. Pei-Ling, S. Yu-Han, T. Hui-Ting, W. Kuo-Ching, Determination of Marked Components-aloin and aloe-emodin in Aloe vera before and after hydrolysis, J. Food Drug Anal. 20 (2012) 646–654.
[15] X.Y. Dai, W. Nie, Y.C. Wang, Y. Shen, Y. Li, S.J. Gan, Electro spun emodin poly (vinyl pyrrolidone) blended nanofibrous membrane: a novel medicated biomaterial for drug delivery and accelerated wound healing, J. Mater. Sci. - Mater. Med. 23 (2012) 2709–2716.
[16] T.A. Syed, S.A. Ahmad, A.H. Holt, S.A. Ahmad, S.H. Ahmad, M. Afzal, Management of psoriasis with Aloe vera extract in a hydrophilic cream: a placebo-controlled, double-blind study, Trop. Med. Int. Health 1 (1996) 505–509.
[17] J. Gibson, An evaluation of the effects on ProZ92 on proliferation of skin cells in culture, <www.proz92.com/psoriasis/research> (Cited 16.01.14).
[18] A. Yogeeta, C.P. Kailash, K.S. Krutika, Development, evaluation and clinical studies of Acitretin loaded nanostructured lipid carriers for topical treatment of psoriasis, Int. J. Pharm. 401 (2010) 93–102.
[19] A. Sharma, T. Garg, A. Aman, K. Panchal, R. Sharma, S. Kumar, T. Markandeywar, Nanogel–an advanced drug delivery tool: current and future, Artif. Cells Nanomed. Biotechnol. 44 (2016) 165–177.
[20] R. Jayakumar, N. Amrita, R.N. Sanoj, S. Maya, S.V. Nair, Doxorubicin-loaded pH-responsive chitin nanogels for drug delivery to cancer cells, Carbohyd. Polym. 87 (2012) 2352–2356.
[21] R.N. Sanoj, R. Ranjusha, B. Avinash, M. Nishil, R. Jayakumar, Gold–chitin–manganese dioxide ternary composite nanogels for radio frequency assisted cancer therapy, RSC Adv. 4 (2014) 5819–5825.
[22] H. Tamura, H. Nagahama, S. Tokura, Preparation of hydrogels under mild conditions, Cellulose 13 (2006) 357–364.
[23] M. Sabitha, R.N. Sanoj, N. Amrita, L. Vinothkumar, S.V. Nair, R. Jayakumar, Curcumin loaded chitin nanogels for skin cancer treatment via the transdermal route, Nanoscale 4 (2012) 239–250.
[24] R. Jayakumar, H. Tamura, Synthesis, characterization and thermal properties of chitin-g-poly (ε-caprolactone) copolymers by using chitin gel, Int. J. Biol. Macromol. 3 (2008) 32–36.
[25] M. Sabitha, R.N. Sanoj, N. Amrita, L. Vinoth kumar, S.V. Nair, R. Jayakumar, Development and evaluation of 5-flouorouracil loaded chitin nanogels for treatment of skin cancer, Carbohydr. Polym. 91 (2013) 48–57.
[26] R.N. Sanoj, N. Amrita, M. Sabitha, K.P. Chennazhi, H. Tamura, S.V. Nair, R. Jayakumar, Synthesis, characterization and in vitro cytocompatibility studies of chitin nanogels for biomedical applications, Carbohydr. Polym. 93 (2012) 936–942.
[27] K.T. Smitha, A. Anitha, T. Furuike, H. Tamura, S.V. Nair, R. Jayakumar, In vitro evaluation of paclitaxel loaded amorphous chitin nanoparticles for colon cancer drug delivery, Colloids. Surf. B. Biointerfaces 104 (2013) 245–253.
[28] R.K. Farag, R.R. Mohamed, Synthesis and characterization of carboxymethyl chitosan nanogels for swelling studies and antimicrobial activity, Molecules 18 (2012) 190–203.
[29] P.P. Shah, P.R. Desai, A.R. Patel, M.S. Singh, Skin permeating nanogel for the cutaneous co-delivery of two anti-inflammatory drugs, Biomaterials 33 (2012) 1607–1617.
[30] B.P. Ravi, S. Luis, W. Hanping, K. Tianyi, A.E. Agata, Effect of injection site on *in situ* implant formation and drug release *in vivo*, J. Control. Release 147 (2010) 350–358.
[31] D. Ashish, C.M. Jithin, V. Sreeja, H. Tamura, S.V. Nair, R. Jayakumar, Novel carboxymethyl chitin nanoparticles for cancer drug delivery applications, Carbohydr. Polym. 79 (2010) 1073–1079.
[32] J. Smith, E. Wood, M. Dornish, Effect of chitosan on epithelial cell tight junctions, Pharm. Res. 21 (2004) 43–49.
[33] L. Hao, J. Chan, T. Ying, W. Fude, M.Y.Y. Chunwang, Cytotoxicity of silica nanoparticles on HaCaT cells, J. Appl. Toxicol. 34 (2014) 367–372.
[34] S. Daoud-Mahammed, P. Couvreur, R. Gref, Novel self-assembling nanogels: stability and lyophilisation studies, Int. J. Pharm. 332 (2007) 185–191.
[35] J.R. Laxmi, R. Karthikeyan, B.P. Srinivasa, R.V.V. Narendra Babu, Formulation and evaluation of antipsoriatic gel using natural excipients, J. Acute Dis. 2 (2013) 115–121.
[36] A. Vijayalakshmi, V. Ravichandiran, V. Malarkodi, S. Nirmala, M. Anusha, S. Jayakumari, K. Masilamani, Anti-psoriatic activity of Smilax China Linn. Rhizome, Ind. J. Pharm. Edu. Res. 47 (2013) 82–89.
[37] S. Manmohan, K. Niraj, L. *Cassia tora* L. Creams inhibit psoriasis in mouse tail model, Pharm. Crop 3 (2012) 1–6.
[38] A. Nagle, A.K. Goyal, R. Kesarla, R.S.R. Murthy, Efficacy study of vesicular gel containing methotrexate and menthol combination on parakeratotic rat skin model, J. Liposome Res. 21 (2011) 134–140.
[39] S. Khurana, N.K. Jain, P.M. Bedi, Nanostructured lipid carriers based nanogel for meloxicam delivery: mechanistic, in-vivo and stability evaluation, Drug Dev. Ind. Pharm. 8 (2015) 1368–1375.
[40] A. Inmaculada, M. Marian, H. Ruth, P. Ines, M. Beatriz, A. Niuris, G. Gemma, H. Angeles, Functional characterization of chitin and chitosan, Curr. Chem. Biol. 3 (2009) 203–230.
[41] A.E. Stuck, C.J. Brindley, A. Busslinger, F.J. Frey, Pharmacokinetics of acitretin and its 13-cis metabolite in patients on haemodialysis, Br. J. Clin. Pharmacol. 27 (1989) 301–304.
[42] M. Chaitanya, B. Babajan, M. Naveen, P. Madhusudana, C.M. Anuradha, K.C. Suresh, Design and evaluation of new chemotherapeutics of aloe-emodin (AE) against the deadly cancer disease: an in silico study, J. Chem. Biol. 6 (2013) 141–153.
[43] T.R. Arunraj, R.N. Sanoj, N. Ashwin Kumar, R. Jayakumar, Bio-responsive chitin-poly(L-lactic acid) composite nanogels for liver cancer, Colloids Surf. B. Biointerfaces 113 (2014) 394–402.
[44] P. Desai, R.R. Patlolla, M. Singh, Interaction of nanoparticles and cell-penetrating peptides with skin for transdermal drug delivery, Mol. Membr. Biol. 27 (2010) 247–259.
[45] L. Xin, L. Hai-Shu, J.C. Thenmozhiyal, Y.C. Sui, C.H.O. Paul, Inclusion of acitretin into cyclodextrins: phase solubility, photostability, and physicochemical characterization, J. Pharm. Sci. 9 (2003) 2449–2457.
[46] T. Brijesh, B. Rohit, P. Alka, G. Jitender, C. Gautam, W. Suresh, H.C. Eun, A. Pankaj, Potential antioxidant anthraquinones isolated from rheum emodi showing nematicidal activity against meloidogyne incognita, J. Chem. 1 (2014) 1–9.
[47] L. Malpezzi, G.A. Magnone, N. Masciocchi, A. Sironi, Single crystal and powder diffraction characterization of three polymorphic forms of Acitretin, J. Pharm. Sci. 94 (2005) 1067–1078.
[48] S. Wang, T. Chen, R. Chen, Y. Hu, M. Chen, Y. Wang, Emodin loaded solid lipid nanoparticles: preparation, characterization and antitumor activity studies, Int. J. Pharm. 430 (2012) 238–246.
[49] N. Sanoj Rejinold, M. Muthunarayanan, V.V. Divyarani, P.R. Sreerekha, K.P. Chennazhi, S.V. Nair, H. Tamura, R. Jayakumar, Curcumin-loaded biocompatible thermo responsive polymeric nanoparticles for cancer drug delivery, J. Colloid Interface Sci. 360 (2011) 39–51.
[50] S.B. Murray, A.C. Neville, The role of pH, temperature and nucleation in the formation of cholesteric liquid crystal spherulites from chitin and chitosan, Int. J. Biol. Macromol. 22 (1998) 137–144.
[51] W. Xu, P.A. Ledin, F.A. Plamper, C.V. Synatschke, A.H.E. Müller, V.V. Tsukruk, Multi responsive microcapsules based on multilayer assembly of star polyelectrolytes, Macromolecules 47 (2014) 7858–7868.
[52] G.M.G. Chiara, F. Silvia, P. Sara, C. Emanuela, V. Giulio, M. Luisa, M. Paola, C. Francesco, Skin penetrating peptide as a tool to enhance the permeation of heparin through human epidermis, Biol. Macromol. 17 (2016) 46–55.

[53] I. Harhaji, A.M. Sanja, M.I. Danijela, P. Dusan, I. Aleksandra, T.M. Biljana, Aloe-emodin inhibits the cytotoxic action of tumor necrosis factor, Eur. J. Pharmacol. 568 (2007) 248–259.
[54] S. Mijatovic, D. Maksimovic-Ivanic, J. Radovic, D.J. Miljkovic, L.J. Harhaji, O. Vuckovic, S. Stosic-Grujicic, S.M. Mostarica, V. Trajkovic, Anti-glioma action of aloe- emodin: the role of ERK inhibition CMLS, Cell. Mol. Life Sci. 62 (2005) 589–598.
[55] P. Dusan, S. Emina, R. Zorica, D. Vladimir, T. Vladimir, M. Ljiljana, P. Svetlana, Aloe-emodin inhibits proliferation of adult human keratinocytes in vitro, J. Cosmet. Sci. 63 (2012) 297–302.
[56] G. Miroslav, K. Birgit, N. Michael, D. Elisabeth, W. Martina, M. Barbara, K. Julia, G. Teresa, P. Dagmar, B. Karl, B. Markus, P. Alexander, W. Christoph, Tetrahydro anthraquinone Derivative (±)-4-Deoxyaustrocortilutein Induces Cell Cycle Arrest and Apoptosis in Melanoma Cells via Up regulation of p21 and p53 and Down regulation of NF-kappaB, J. Cancer 7 (2016) 555–568.
[57] S. Gottlieb, E. Hayes, P. Gilleaudeau, I. Cardinale, A.B. Gottlieb, J.G. Krueger, Cellular actions of etretinate in psoriasis: enhanced epidermal differentiation and reduced cell-mediated inflammation are unexpected outcomes, J. Cutan. Pathol. 23 (1996) 404–418.
[58] P. Dupuy, M. Bagot, M. Heslan, L. Dubertret, Synthetic retinoids inhibit the antigen presenting properties of epidermal cells in vitro, J. Invest. Dermatol. 93 (1989) 455–459.
[59] T. Min-Lang, C. Rong-Huei, B. Shi-Wei, C. Wei-Yu, The storage stability of chitosan/tripolyphosphate nanoparticles in a phosphate buffer, Carbohydr. Polym. 84 (2011) 756–761.
[60] H.C. Pal, J.C. Chamcheu, V.M. Adhami, G.S. Wood, C.A. Elmets, H. Mukhtar, F. Afaq, Topical application of delphinidin reduces psoriasiform lesions in the flaky skin mouse model by inducing epidermal differentiation and inhibiting inflammation, Br. J. Dermatol. 172 (2015) 354–364.
[61] E.G. Johann, J. Andrew, D. Melissa, Mouse models of psoriasis, J. Invest. Dermatol. 127 (2007) 1292–1308.
[62] H. Nakaguna, T. Kambara, T. Yamamoto, Rat ultravoilet ray B photodermatitis: an experimental model of psoriasis vulgaris, Int. J. Exp. Pathol. 76 (1995) 65–73.
[63] A.G. Soboleva, A.V. Mezentsev, S.A. Bruskin, Genetically modified animals as model systems of psoriasis, Mol. Biol. (Mosk) 48 (2014) 587–599.